

THERMAL CYCLING FATIGUE IN DIPS MOUNTED WITH EUTECTIC
TIN-LEAD SOLDER JOINTS IN STUB AND GULL WING GEOMETRIES

A paper for consideration for the 1993 International Telemetering
Conference, Riviera Hotel and Convention Center, Las Vegas, NV,
October 25- 28, 1993

by

J.W. Winslow and C. de Silveira, 103-100, Jet Propulsion Laboratory,
California Institute of Technology, Pasadena, CA 91109

I. DESCRIPTION OF THE PROBLEM

For many decades it has been known that mechanical strength in
solders is subject to failure under mechanical stress. In early electronic
systems, such failures were avoided primarily by not using solder as a
mechanical structural component. The rule was first to make sound
wiring connections, mechanically independent of the solder, and only then
to solder them.

With miniaturization resulting from use of modern solid state electronic components and Printed Wiring Boards (PWBS), that old rule of thumb has gone by the board. Careful design of modern electronic systems limits the mechanical stresses exerted on solder joints to values less than their yield strengths, and these joints have become integral parts of the mechanical structures. This practice has become particularly widespread in circuitry intended for use in spacecraft, where the premium for reduction of mass is especially high.

While these joints are strong when new, some of them have shown failure due to fatigue as they age. These fatigue failures have restricted the useful lifetimes of their circuits to values which are undesirably short, especially in the case of long mission spacecraft. This is particularly annoying because details of the fatigue mechanism(s) are poorly understood, resulting in large uncertainties when predicting lifetimes, and requiring correspondingly large safety margins in the design of electronic hardware.

II. PREVIOUS RESEARCH

Over recent decades, fatigue mechanisms in solders have attracted the attentions of many researchers. Many different solders have been studied, with different solders behaving rather differently from one another. For a while it seemed that whatever the result of one life study, another soon would come along to refute it. Consequently, we early opted for the relatively simple case of a single composition, namely near-eutectic tin-lead solder; i.e. about three atoms of tin for each atom of lead (by weight, 63% Sn/37% Pb).

Secondly, previous studies have shown that solder fatigue failures in general are associated with changes in temperature of the hardware, presumably via stresses and/or strains arising from differential thermal expansion between its various mechanical components. In this respect we remember the "instant-on" TV set had a considerably improved reliability, albeit at the cost of higher electric bills, through reducing the number of thermal cycles experienced by the hardware during a service lifetime.

Finally, many NASA mission orbits have periods, and thus temperature cycles that are relatively slow, i.e. on the order of 90 minutes to 24 hours (or more) per cycle. Previous researchers have shown that in such slowly changing environments the phenomenon of creep plays an important role in solder fatigue.

III. BASIC MECHANISMS

We consider the doctoral thesis of Frear⁽¹⁾ especially illuminating with respect to the thermal cycling degradation of near-eutectic tin-lead solder. In the section of this thesis treating such solder, he notes the existence of time- and temperature-dependent "grain coarsening" in this two-phased material. That is, the alpha phase (lead-rich) inclusions in the beta phase (tin-rich) matrix, become both larger and farther apart, as the joint ages. The same tendency also is reported by Ross⁽²⁾, who further reports that in each of the two phases the Pb and Sn atoms monotonically segregate from each other with time and temperature. (See Fig 1 and Table I.)

Frear also notes that certain interior regions of the near-eutectic, Sn-Pb solder joint display grain coarsening which is markedly enhanced beyond the average for the joint as a whole (See Fig 2). These regions are of special interest because solder joint fracture occurs within them. Similar observations of increased coarsening in selected regions within a thermal cycled joint, and co-location of the cracked region, also have been reported by others (for example see Fig 3, Frankland et al (3)).

Since thermal diffusivity for tin-lead solder is relatively high, and since thermal cycling reverses any possible temperature gradients that might exist, it seems rather unlikely that such enhanced coarsening can be attributed simply to prolonged higher temperatures in the affected regions. We conclude rather that this enhancement probably corresponds to regions where the solder has been strained (by creeping) during thermal cycling. Whether this effect results from enhanced diffusion along grain boundaries, or is more a sort of "stirring" effect the result would be to bring lead atoms into contact with each other at a much faster rate than does simple diffusion, with a consequently faster growth of the alpha phase inclusions.

Finally, Frear reports the presence of small intraphase cracks in the beta phase regions when the grain coarsening has proceeded far enough (See Fig 4). This suggests that the mechanical properties of the tin-rich regions change as their compositions and dimensions change, until these regions no longer can sustain the stresses provided by the thermal cycling environment. In this circumstance, with continued cycling, the small cracks could grow until they linked up with each other, eventually leading to separation of the joint.

Putting these observations together, we concur with Frear that a three-step degradation mechanism applies to eutectic tin-lead solder under thermal cycling environments. First, grain coarsening and atomic Pb-Sn segregation proceed until the alpha phase inclusions are separated by beta phase regions too large and too brittle to support the stresses imposed by the environment. Then, microcracks initiate in the beta-phase regions. Finally, as thermal cycling continues, the cracks grow until they join with each other to separate the joint.

IV. EXPERIMENTAL INVESTIGATION

Investigation of such a complicated mechanism poses too many practical difficulties to be discussed in detail today. However, as a first step we have conducted one experimental investigation which may offer a small degree of illumination.

Elsewhere (4) it was proposed that accelerated thermal cycle test results might be extrapolated to service environments using the relationship

where

L_S is the estimated lifetime of the service solder joints,

L_T is the lifetime observed for the solder joints in the accelerated test,

ΔT_T is the temperature range ($= T_{max} - T_{min}$) for the accelerated test cycle, and

ΔT_S is the temperature range for the service environment.

This equation is a simplified version of the Coffin-Manson equation, where the value of the exponent was determined empirically from data given in previous literature. It is of interest to note that this relationship predicts that reducing ΔT by a factor of two should increase the predicted lifetime by a factor of about six.

The experiment designed for this study was a straight-forward test of this proposed relationship, using identical specimens under several thermal cycling environments, each such environment having its own value of ΔT .

EXPERIMENTAL DESIGN

To date, our experimental investigation has subjected identical test articles, each consisting of (a) five stub-mounted (sometimes call butt-joined), 14 lead DIPs, and (b) five gull-wing mounted 14 lead DIPs, on a PWB (see Fig 5), to two different thermal cycles. Tensile-compressive mechanical forces were exerted on the solder joints via a conformal coating material encapsulating the DIPs, filling the entire gap between each DIP ceramic body and its PWB. This configuration provided larger than usual driving forces due to the mismatches between coefficients of thermal expansion (CTEs) of the coating material, the DIP leads, the component body, and the PWB.

Please note that these Test Articles are flight-like in design and assembly, and were assembled by flight-trained assembly technicians. However, permitting the conformal coating to fill the 60-mil gap between PWB and component body is in direct violation of the normal procedure for coating a PWB. This was done to accelerate the degradation of the joints. The Test Articles thus do not represent actual flight quality hardware.

EXPERIMENTAL DETAILS

To date, two main thermal cycles have been used. Oven temperatures of these cycles are given in Fig 6.

Failure of each specimen was defined by an electrical continuity loss event detector (5). For each DIP the leads were daisy-chained together through a set of electrical connections involving shorting wires between the lead shoulders, and between solder pad lands on the PWBS.

Unfortunately, the event detector proved vulnerable to electrical noise from our ovens, so that false signals were numerous when our test articles were unshielded. With careful attention to shielding of test articles and the cables connecting them to the detector, these false signals were reduced in number to a reasonable level. However, it still was necessary to pay close attention to event indications over several consecutive cycles to identify electrical continuity loss with reasonable certainty.

V. EXPERIMENTAL RESULTS

For stub mounted DIP specimens, the number of cycles to failure was found almost independent of temperature range ΔT (see Fig 7). That is, the ratio of about 6 predicted by the proposed extrapolation relationship between the lifetimes for the two values of ΔT , was conspicuous by its 'absence. For the case of our gull-wing mounted DIPs, the story was quite different (see Fig 8). Here "the number of cycles to failure for the smaller value of ΔT was roughly three times that found for the larger ΔT .

V1. DISCUSSION OF RESULTS

We have noted in the past that solder joints in the gull-wing configuration, when thermal cycled, show surface cracks in the solder that first appear around the heel of the joint. Then, as thermal cycling continues, the cracks propagate along both sides of the lead foot until they reach the toe area. Then, the lead separates from the solder pad, as shown in Fig. 9.

Figures 10 & 11 show scanning electron microscope (SEM) photos of cross sections of two leads (Nos 6 & 9) of one of our gull-wing mounted DIPs, taken some two cycles after failure as defined by our event detector criteria. We note that lead #9 has separated completely from its solder pad, while lead #6 (directly across the DIP from #9) has separated from its pad along most of the length of the foot from the heel toward the toe, but remains attached at the toe.

Based on the above observations, we speculate that the two DIP configurations fail by different mechanisms. To us it appears that the stub-mounted DIPs fail primarily by simple tensile failure of the solder, while failure of the gull-wing configuration is dominated by crack propagation through the solder, parallel to the foot.

From our point of view, the significance of these results lies in the observation that the failure mode depends upon joint geometry. This suggests that by careful tailoring of the joint, we may be able to collect experimental data illuminating different phases of the failure mechanism. For example, we may be able to quantify the crack growth step by use of gull-wing joint data, and the crack initiation step by using data from stub-mounted specimens.

However, these results must be considered only as preliminary, with much work yet to be done in verifying and expanding the ideas reported here. It will take much more effort before fatigue failures in this material can be considered as under practical control. Also, it must be pointed out that other solders may behave differently. Frear, for example, reports that for 95-5 lead-tin solder, grain structure appears to refine, rather than coarsen, with age.

This research was performed at the Jet Propulsion Laboratory of the California Institute of Technology, Pasadena CA, under a contract with the National Aeronautics and Space Administration.

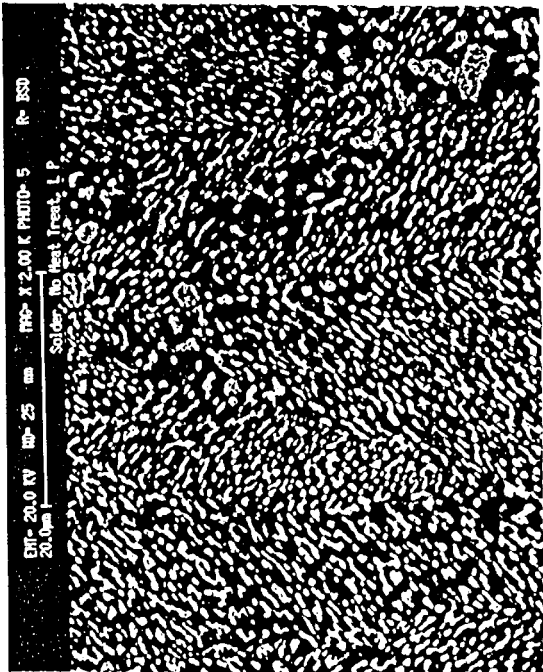
REFERENCES

1. Frear, D.R. 1987 "Microstructural Observations of the Sn-Pb Solder/Cu System and Thermal Fatigue of the Solder Joint", PhD Thesis U Calif, Berkeley, Ca.
2. Ross, R.G. et al, "Creep Fatigue Behavior of Microelectronic Solder Joints", Materials Research Society Symposium Proceedings, Mechanical Behavior of Materials and Structures in Microelectronics, 1991 MRS Spring Meeting, Anaheim CA, 30 Apr -4 May, 1991.
3. Frankland, H. G., Sanderson, I., Sawyer, N. J., & Crownhart, C. 1969, "Final Report for LM Landing Radar, Solder Joint Research Program, Improving the Reliability of Stud Type Solder Joints" Ryan Aeronautical Co. Report No. 53969-55, dated 15 April 1969.
4. JPL Publication 89-35, "Magellan/Gallileo Solder Joint Failure Analysis & Recommendations", by Ronald G. Ross Jr, dated September 15, 1989.
5. Event Detector, Analysis and Technology, Inc. Model No. 128

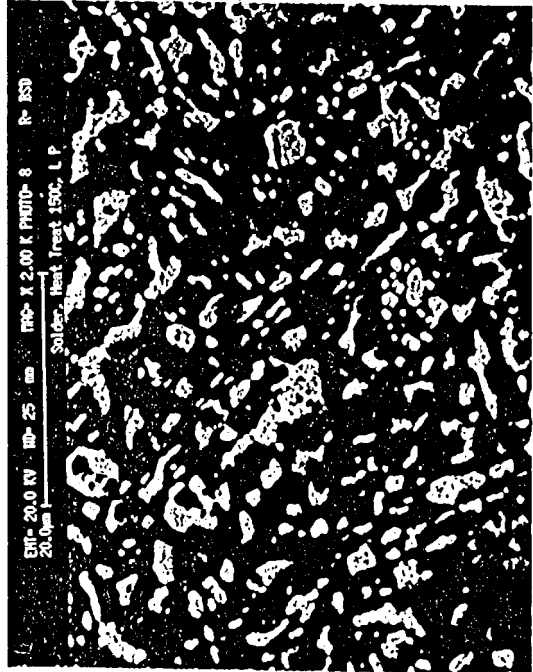
FIGURE CAPTIONS

- FIG 1. SEM Photos of Aged Microstructure, Eutectic Tin-Lead Solder
(from Ross et al⁽²⁾)
- FIG 2. Optical Microphoto of Near-Eutectic Tin-Lead Solder after
Thermal Cycling (after Frear⁽¹⁾)
- FIG 3. Optical Microphoto of Eutectic Tin-Lead Solder after
Thermal Cycling (after Frankland et al ⁽³⁾)
- FIG 4. Polarized Optical Microphoto of Near-Eutectic Tin-Lead Solder
after Thermal Cycling. Intragranular Cracks through Beta
Phase indicated by arrows. (after Frear⁽¹⁾)
- FIG 5. Test Article 24A
- FIG 6. Thermal Cycles (oven programs)
- FIG 7. First-pin Failures for Stub-mounted DIPs,
- FIG 8. First-pin Failures for Gull-wing Mounted DIPs.
- FIG 9, SEM Photos of DIP Leads about 205 Thermal Cycles after First-
pin Failure.
- FIG 10. SEM Photos of X-sectioned Lead #9, Specimen TA24D-2,
S/N144, about 2 Thermal Cycles after First-pin Failure.
- FIG II. SEM Photos of X-sectioned Lead #7, Specimen TA24D-2,
S/N144, about 2 Thermal Cycles after First-pin Failure.

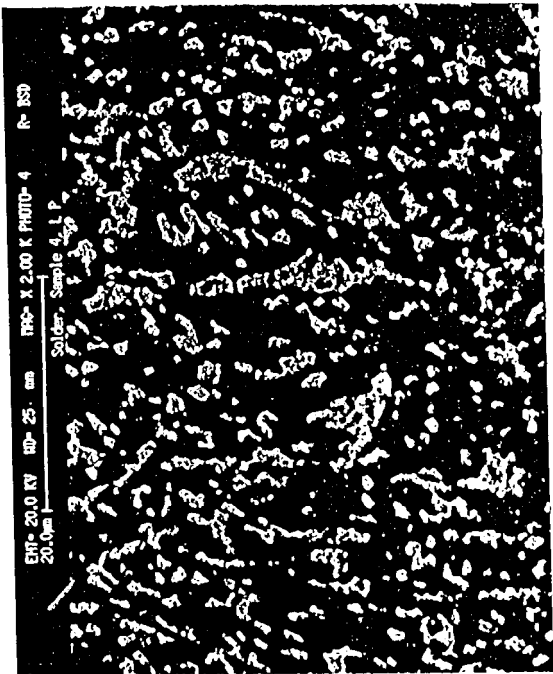
← 20 μm →



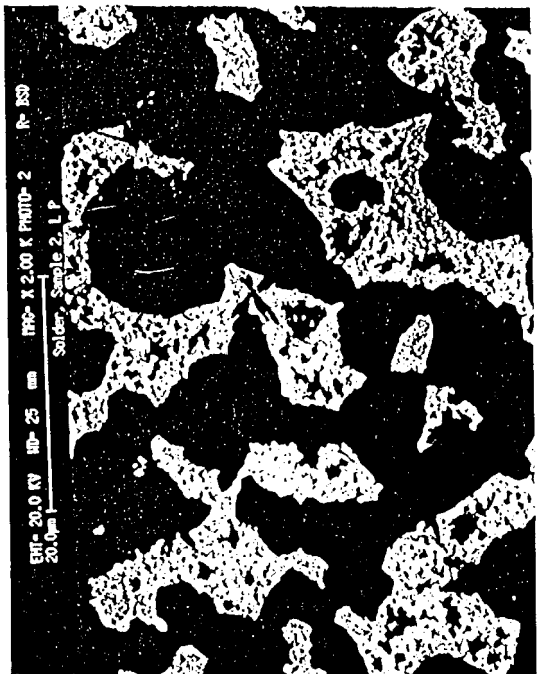
1a Immediately after solidifying



1b after 10 hrs at 150 °C



1c after 5 hrs at 100 °C

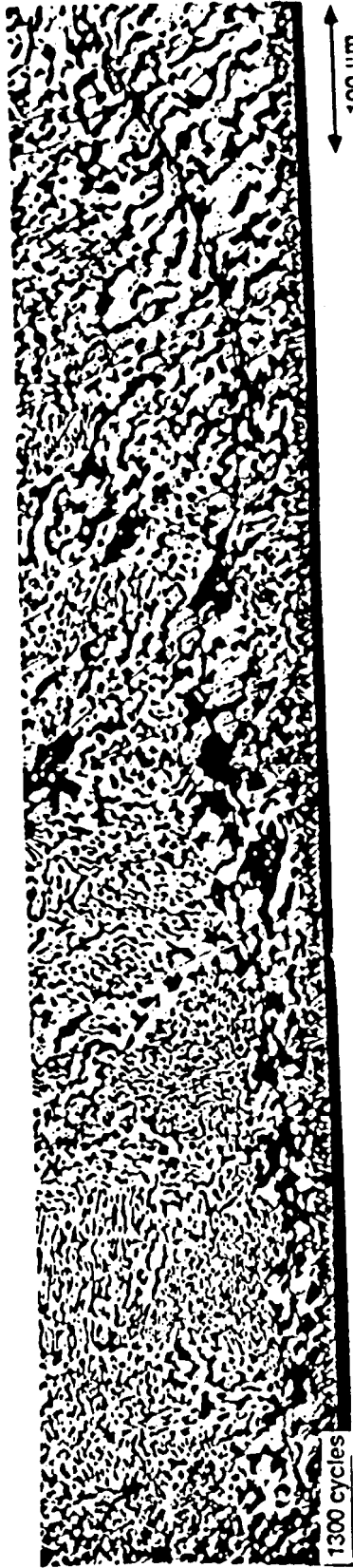


1d after 5 hrs at 100 °C

Fig 1. SEM Photos of Aged Solder. (From Pass (2))

Table 1. Solder Metallurgical Properties Measured on Cross-sectioned Solder Joints of Various Ages and Thermal Exposure Histories (after Ross⁽¹⁾)

Sample Aging History	Grain Size (microns)	Lead-rich Phase		Tin-rich Phase	
		% Pb	% Sn	% Sn	% Pb
Just soldered	1.17	71.2	28.8	80.4	19.6
10 hours @ 150°C	2.97	79.3	20.7	97.9	2.1
6 hours @ 100°C	1.42	83.3	16.7	91.5	8.5
1.5 years @ 23°C	2.08	97.3	2.7	96.9	3.1
15 years @ 23°C (Viking '75)	8.76	97.6	2.4	99.9	0.1
18 years @ 23°C (MVM '73)	9.03	98.3	1.7	100.	0.0
24 years @ 23°C (Mariner '67)	9.56	98.6	1.4	99.7	0.3



XBB 8612-10351

Fig 2. Near-Eutectic Tin-Lead Solder after Thermal Cycling
(from Frear ⁶)

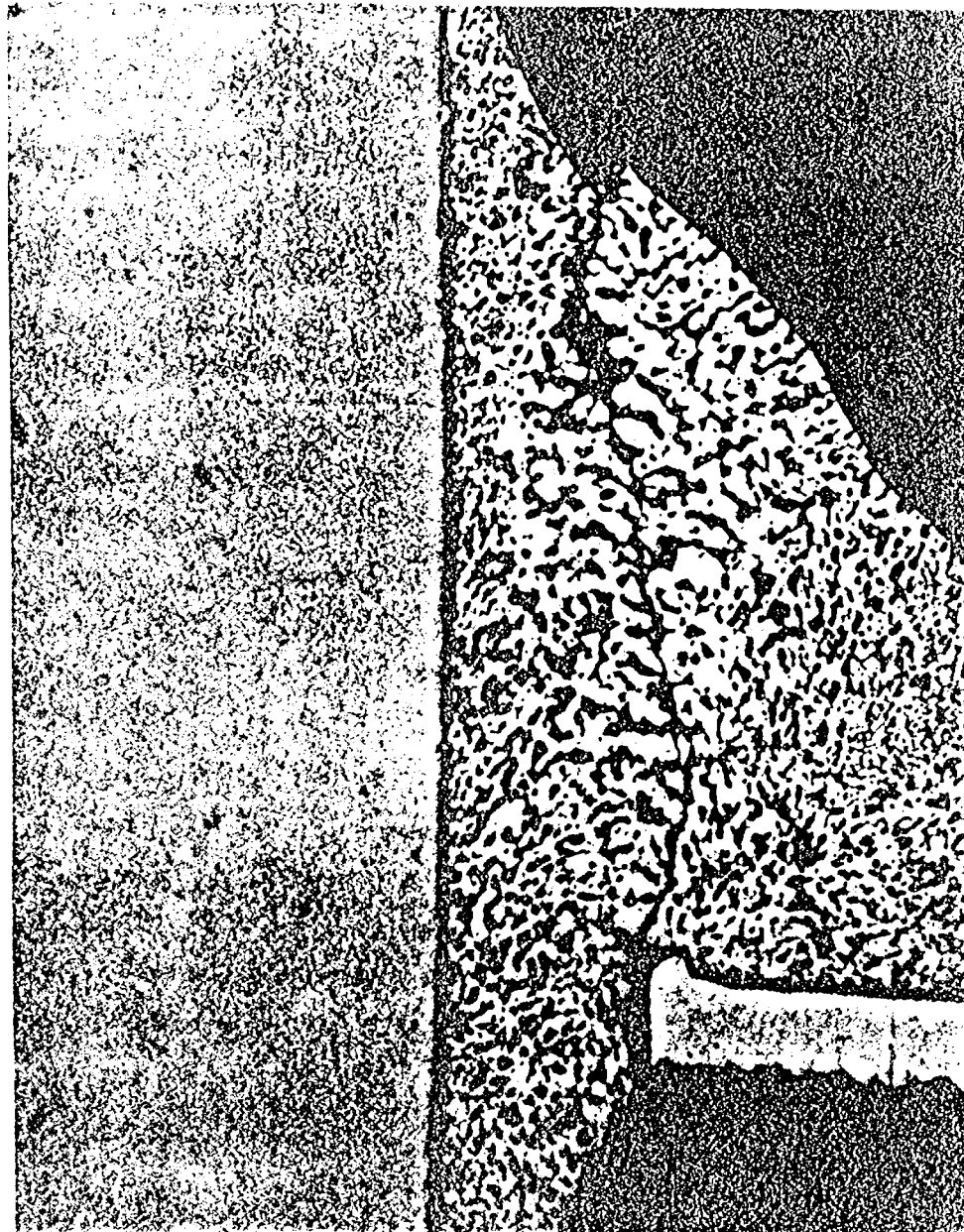


Fig 3 Eutectic Tin-Lead Solder after Thermal Cycling
(from Frankland et al⁽³⁾)



XBB 8612-10349

Figure 4 Polarized optical microstructure cross section of a 60 Sn-40Pb/Cu joint after 1300 cycles. Intergranular cracks through the Sn rich phase are shown.
(From Frear (1))

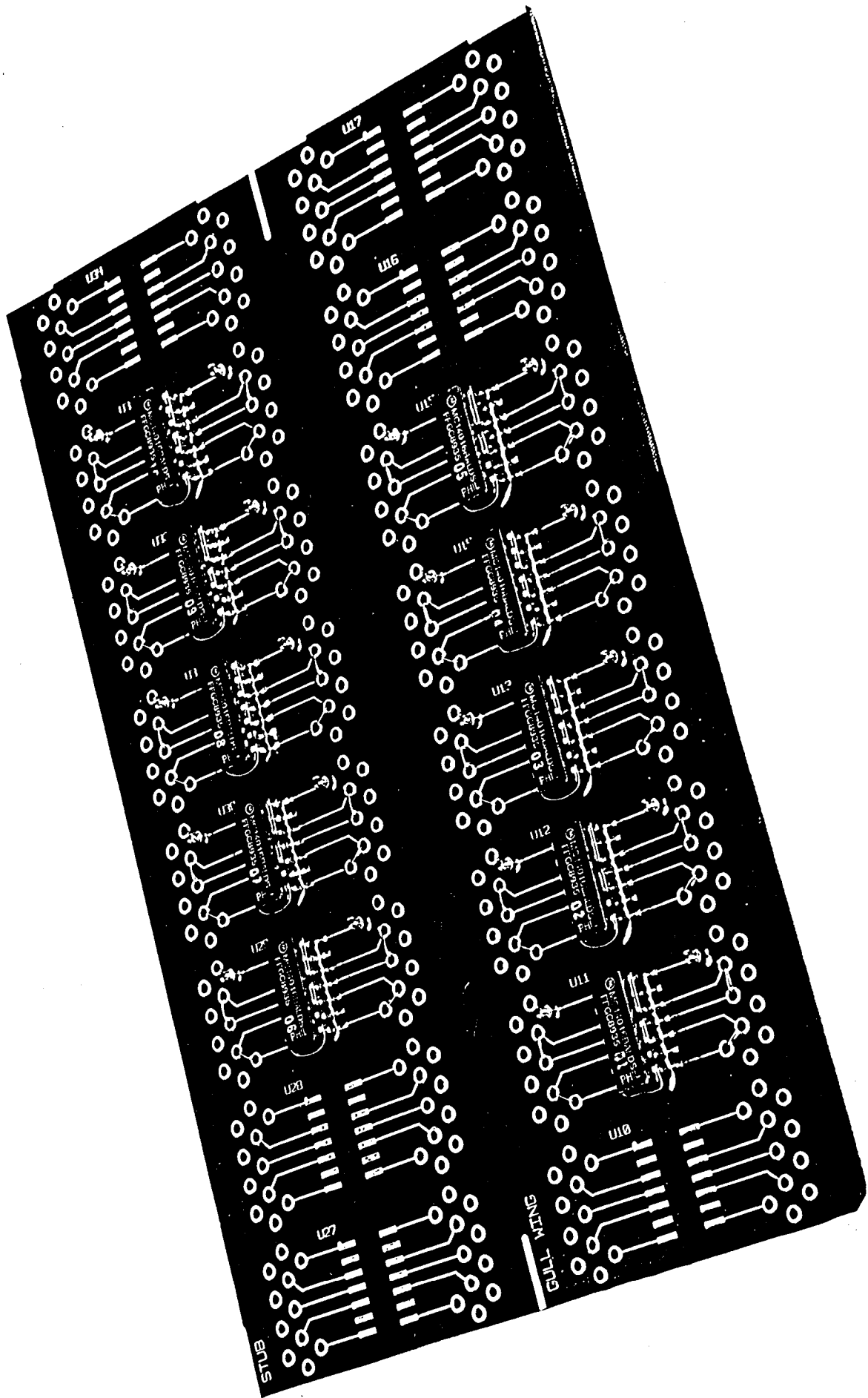


FIG 5. TA24A

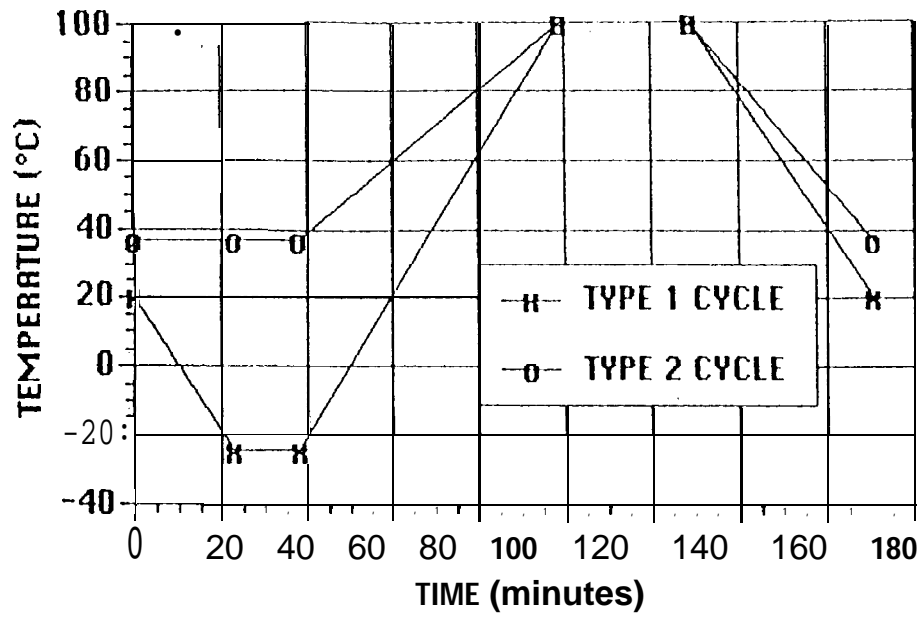


FIG 6. Thermal Cycles

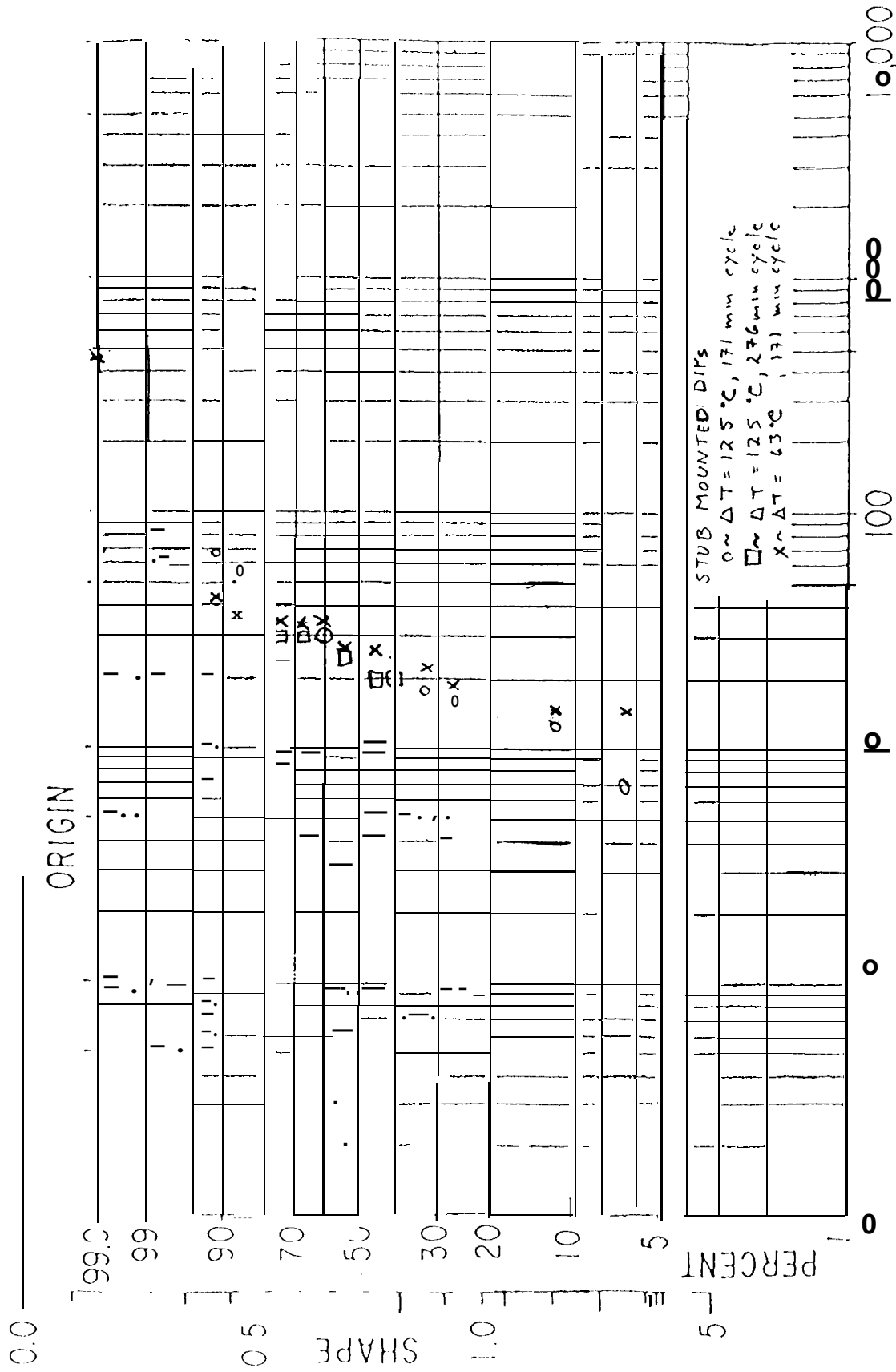
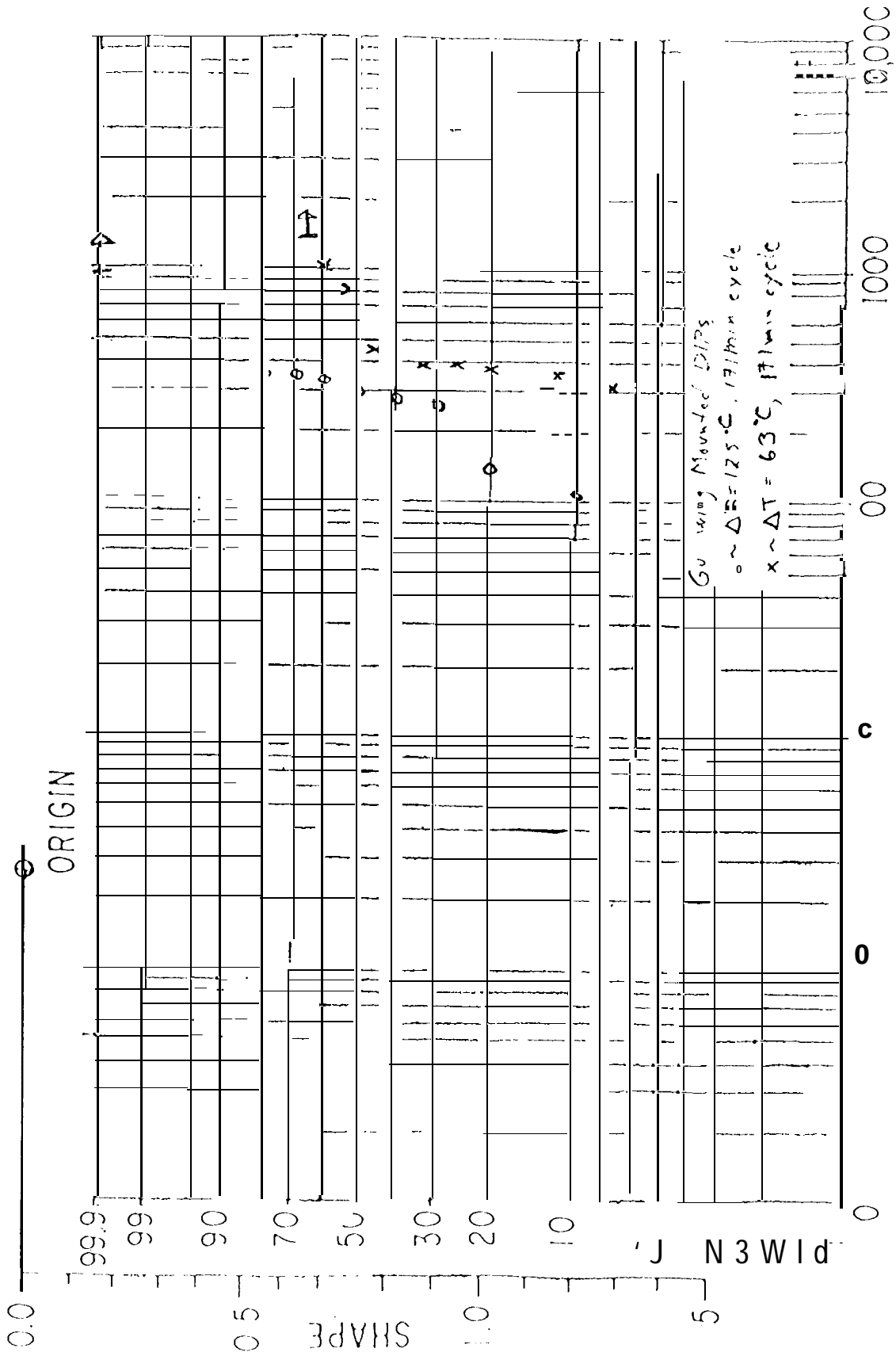
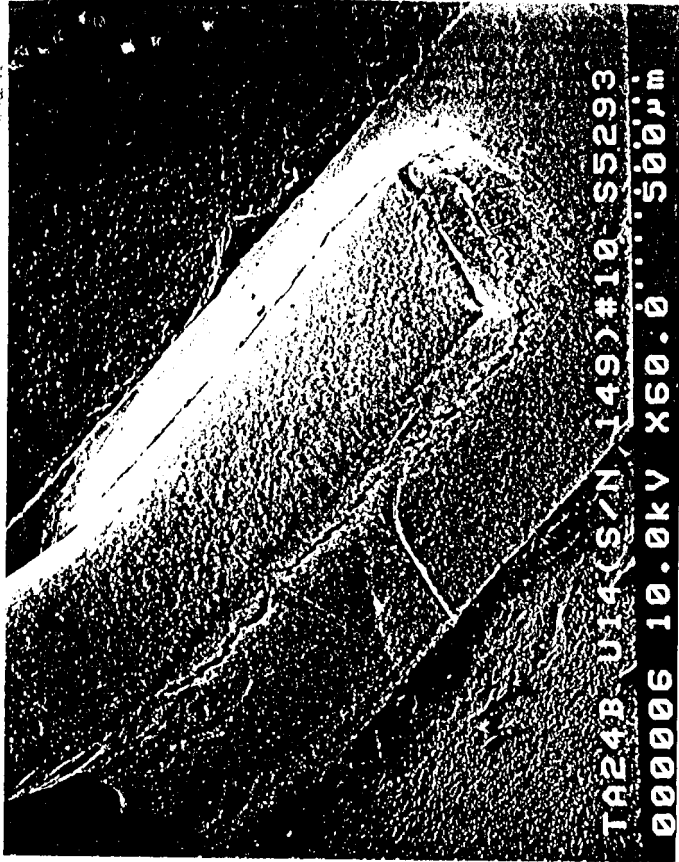


FIG. 7 Failures for stub-mounted DIPs



Failures for Gu wing Mounted DIPs

FIG. 8



69

SEM Photos - DIP leads at about 205
thermal cycles after first pin failure.



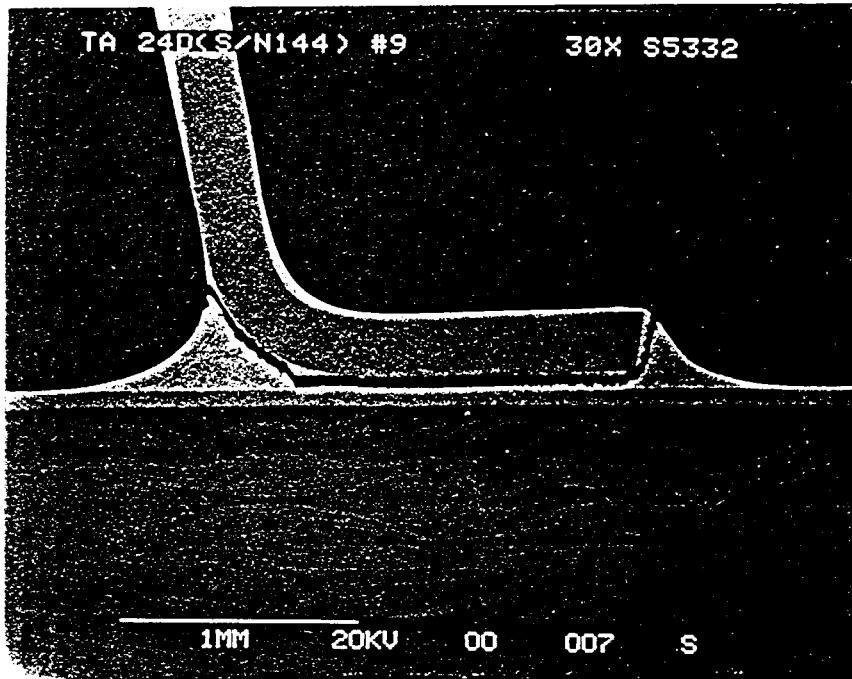


FIG 10

SEM Photos of x-sectioned lead #9, specimen TA24D-2, SN144, at about 2 cycles after failure. Photo after cycle #377, failure at cycle #375.

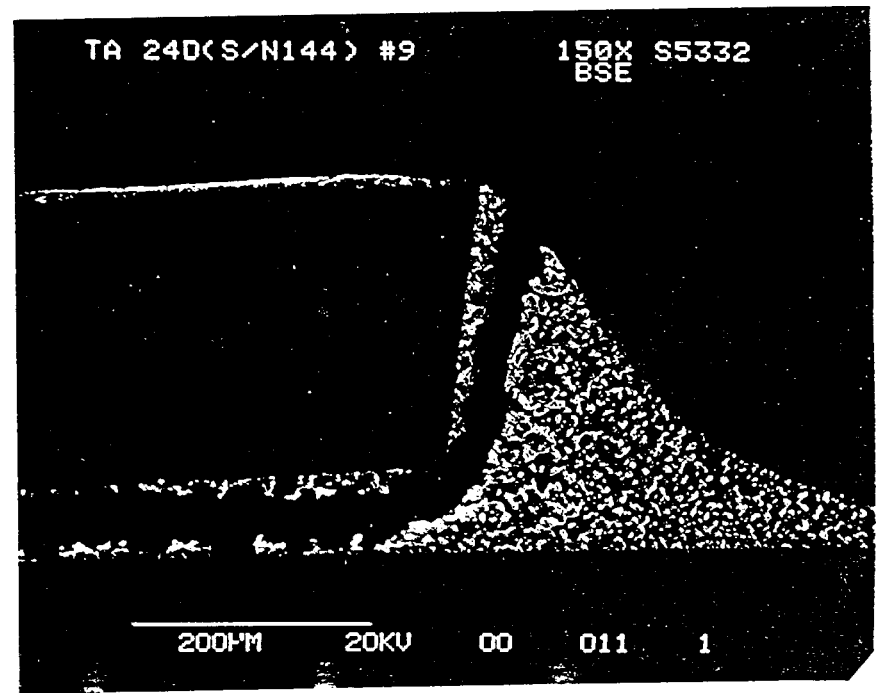
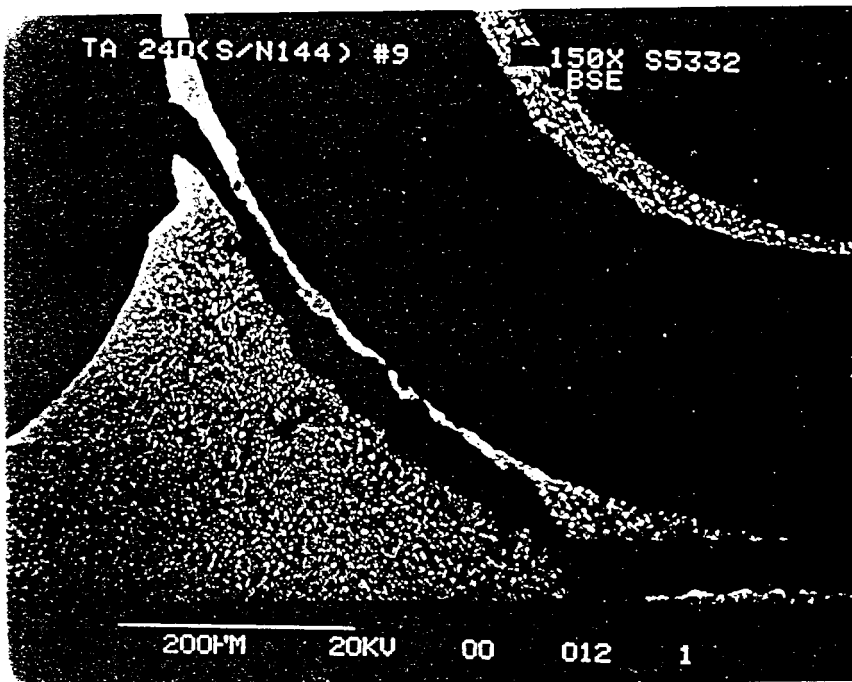


FIG 11

SEM Photos of x-sectioned lead #6,
BIP S/N 144, about 2 cycles after DIP
failure. Photos after cycle #377; failure
at cycle #375.

